Published online 9 November 2022 *Nucleic Acids Research, 2022, Vol. 50, No. 20* **11415–11425**
https://doi.org/10.1093/nar/gkac1023

Amino-acyl tXNA as inhibitors or amino acid donors in peptide synthesis

Lauriane Rietmeyer [1,†], Inès Li De La Sierra-Gallay [2,†], Guy Schepers [3], Delphine Dorchêne [1], Laura Iannazzo [4], Delphine Patin [2], Thierry Touzé [2], Herman van Tilbeurgh [2], Piet Herdewijn [3], Mélanie Ethève-Quelquejeu [4,*] and Matthieu Fonvielle [1,*]

[1]INSERM UMR-S 1138, Centre de Recherche des Cordeliers, Sorbonne Université, Université Paris Cité, F-75006 Paris, France, [2]Institute for Integrative Biology of the Cell (I2BC), CEA, CNRS, Université Paris-Saclay 91198, Gif-sur-Yvette, France, [3]Laboratory of Medicinal Chemistry, Rega Institute for Biomedical Research, KU Leuven, Herestraat 49, Box 1041, 3000 Leuven, Belgium and [4]Université Paris Cité, CNRS UMR 8601, Laboratoire de Chimie et Biochimie Pharmacologiques et Toxicologiques, F-75006Paris, France

Received July 21, 2022; Revised October 17, 2022; Editorial Decision October 18, 2022; Accepted October 21, 2022

ABSTRACT

Xenobiotic nucleic acids (XNAs) offer tremendous potential for synthetic biology, biotechnology, and molecular medicine but their ability to mimic nucleic acids still needs to be explored. Here, to study the ability of XNA oligonucleotides to mimic tRNA, we synthesized three L-Ala-tXNAs analogs. These molecules were used in a non-ribosomal peptide synthesis involving a bacterial Fem transferase. We compared the ability of this enzyme to use amino-acyl tXNAs containing 1′,5′-anhydrohexitol (HNA), 2′-fluoro ribose (2′F-RNA) and 2′-fluoro arabinose. L-Ala-tXNA containing HNA or 2′F-RNA were substrates of the Fem enzyme. The synthesis of peptidyl-XNA and the resolution of their structures in complex with the enzyme show the impact of the XNA on protein binding. For the first time we describe functional tXNA in an *in vitro* assay. These results invite to test tXNA also as substitute for tRNA in translation.

INTRODUCTION

Although chemically modified nucleic acids have long been studied, xenobiotic nucleic acid (XNA) methodology has only recently been introduced, offering new applications in synthetic biology (1). XNAs are chemically modified nucleic acids, of which most have modified carbohydrate moieties and for which the chemistry can be tuned depending on the biological application. In most cases, the chemical modification increases nuclease resistance (2) and improves duplex stability of the XNA (3). In the field of synthetic biology, XNAs have been mainly tested as substitutes for DNA to store and transfer information (4), as aptamers (5,6), and to substitute RNA in biocatalysis (7).

Transfer RNAs are central compounds for the decoding of RNA and bacterial cell-wall synthesis. Here, we investigated the synthesis and function of a tXNA (transfer-XNA) in the context of a tRNA-dependent Fem transferase reaction. The use of tXNA substrates in the reaction represents a new step in the development of synthetic biology based on XNA.

The hexitol nucleic acid (HNA) system provides a noteworthy example of modified oligonucleotide analogs with improved characteristics. HNAs contain the six-membered sugar 1′,5′-anhydro-D-arabino-hexitol instead of the furanose moiety (Figure 1) (2). The 1′,5′-anhydrohexitol nucleoside mimics the natural furanose nucleoside in its 3′-endo conformation, resulting in the axial orientation of the base moiety (8). This feature makes it possible to conformationally pre-organize the single strand HNA oligonucleotide in an A-form, which has been shown to form stable self-complementary duplexes, as well as sequence-selective stable hetero-duplexes with natural DNA and RNA. The A-form character of HNA has been confirmed by NMR studies of a HNA oligomer bound to a complementary RNA oligomer (9) and by X-ray crystallography (10,11). This observation was recently confirmed by studies of a complex between HNA-modified DNA oligonucleotides and an archaeal DNA-polymerase obtained by directed evolution (12). Thus, HNA appears to be a mimic of RNA but has never been used as a functional RNA involving protein catalysis. In the present study, we aimed to evaluate its suitability for the construction of a tXNA.

*To whom correspondence should be addressed. Tel: +33 169084106; Email: matthieu.fonvielle@inserm.fr
†Contributed equally to this work.
Present address: Matthieu Fonvielle, Institute for Integrative Biology of the Cell (I2BC), CEA, CNRS, Université Paris-Saclay, 91198 Gif-sur-Yvette, France.

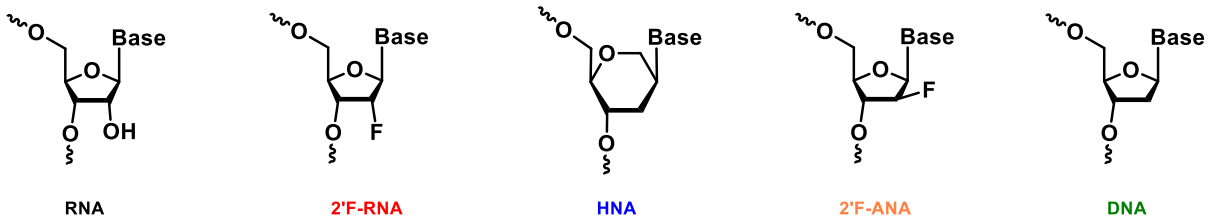

Figure 1. Nucleic acids and xeno-nucleic acids used in this study. RNA: ribonucleic acids (RNA), 2′-deoxy-2′-fluoro ribonucleic acids (2′F-RNA), 1′,5′-anhydrohexitol nucleic acids (HNA), 2′-deoxy-2′-fluoro-D-arabinonucleic acid (2′F-ANA), deoxyribonucleic acids (DNA).

Other XNAs have been designed by replacing the 2′ OH group of RNA or the 2′ H atom of DNA with a fluorine atom (13). The small size of the fluorine substitution leads to minimal steric perturbation in duplex structure formation (14–19). The fluorine can be positioned down or up to the 5-membered cycle (Figure 1), leading to 2′-deoxy-2′-fluoro-ribose (2′F-RNA) as an RNA mimic or 2′-deoxy-2′-fluoro-arabinose (2′F-ANA) as a DNA mimic. The introduction of 2′-Fluoro-RNA residues is known to stabilize duplexes by enhancing the hydrogen bond strength in Watson-Crick type interactions and promoting stacking interactions between bases (20). The high similarity in geometry to RNA (21), the lack of an immunostimulatory effect of fluoro-RNA residues (21), and the increased stability against RNAse (22) make fluoro-RNA an interesting class of XNAs for the design of new bioactive molecules.

In this study, we explored the impact of the XNA modification in aminoacyl-tRNA (aa-tRNA) analogs using HNA or fluoro-RNAs. Aa-tRNAs are substrates of the ribosomal machinery in the synthesis of proteins and are also used in non-ribosomal protein synthesis (NRPS) such as the synthesis of the bacterial cell wall of gram-positive bacteria by Fem transferases (Supplementary Scheme 1) (23), protein degradation by L/F transferases (24), and the modification of bacterial membranes by phosphatidylglycerol synthase (25). Aa-tRNAs are also involved in the synthesis of secondary metabolites, such as cyclodipeptides (26) and natural antibiotics (27).

In our study, we use the Fem transferase enzyme as a model of non-ribosomal peptide synthesis to explore the potential of tXNA analogs. Fem transferases use aa-tRNAs to form branched peptides of the bacterial cell wall peptidoglycan synthesis (see supplementary section 1 and Scheme S1 for details).

We focused on the impact of the incorporation of XNA into the acceptor arm of Ala-tRNA^{Ala}, the substrate of the transferase FemX (Figure 2A). In previous studies, we synthesized analogs of L-Ala-tRNA^{Ala} as substrates of FemX (28) following a strategy described by the group of Hecht (29), which involves the synthesis of aminoacyl-dinucleotides, an enzymatic ligation, and a final deprotection step of the alanine residue (Figure 2B and C). More recently, we synthesized peptidyl-RNA conjugates to obtain high-affinity inhibitors. These peptidyl-RNA conjugates are bi-substrate type analogs in which a peptidoglycan fragment and a RNA moiety are covalently linked by a 1,4-triazole ring. The key chemical step to obtain these molecules is a copper-catalyzed alkyne-azide cycloaddition (CuAAC) between a 2′-azido oligonucleotide (24-nt RNA) and an alkyne-UDP-MurNac-pentapeptide precursor (Figure 3A). These peptidyl-RNA conjugates have shown high inhibitory activity when tested on FemX from *W. viridescens* (30) or FmhB from *S. aureus* (31). Modification of these bi-substrate analogs containing a shorter oligonucleotide (8-nt RNA, Figure 3B) allowed us to solve the first crystallographic structure of a FemX-bi-substrate complex and to identify the protein residues involved in RNA binding and enzymatic transfer (32). Here, we investigated which ribose modifications are tolerated by the NRPS process catalyzed by FemX and we studied the structural features involved in the recognition of XNA fragments by the enzyme.

MATERIALS AND METHODS

Enzyme production and purification

FemX, alanyl-tRNA synthetase, T4 RNA ligase, MurC, MurD, MurE and MurF were produced and purified as previously described (31,32). Protein concentration was determined by the Bradford assay (Biorad) using BSA as a standard.

tRNA production and purification

tRNA^{Ala}(5′-GGGGCCUUAGCUCAGCUGGGAGA GCGCCUGCUUUGCACGCAGGAGGUCAGCGG UUCGAUCCGCUAGGCUCCACCA-3′), corresponding to 76 nt of tRNA^{Ala} of *E. faecalis* strain V583, was obtained by *in vitro* transcription using T7 RNA polymerase (35).

Purification of nucleotide precursors from bacterial extracts

UM5K **5** was purified from vancomycin-susceptible *S. aureus* strain RN4220 as previously described with minor modifications (32) (Supplementary information).

Ligation of *N*-pentenoyl-L-alanyl-dinucleotide (pdCpA-2′-L-Ala-pentenoyl) to 22-nt helices and iodine mediated L-alanyl deprotection

Modified dinucleotide pdCpA-L-Ala-pentenoyl was synthesized, ligated to helices **6a** to **11a** using purified T4 RNA ligase, and deprotected with iodine (36,37) (for details, see supplementary information section 7).

FemX activity in the presence of Ala-tXNAs

The efficiency of the L-alanyl transfer catalyzed by FemX using our tXNA analogs (containing RNA, 2′F-RNA,

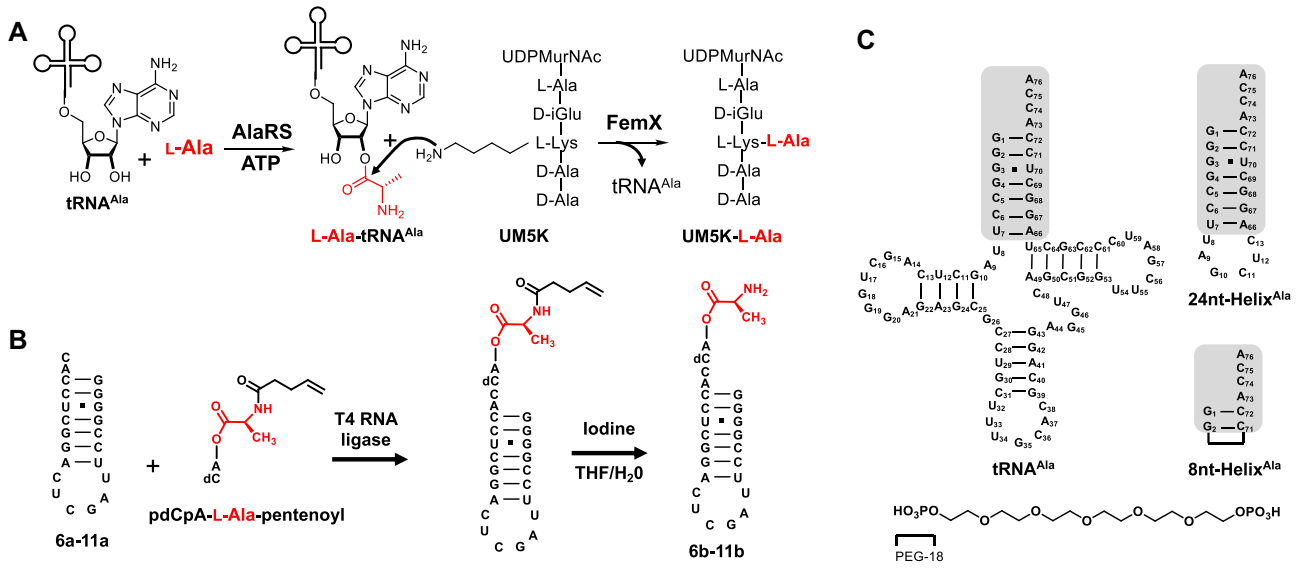

Figure 2. (**A**) Schematic representation of the reaction catalyzed by the alanyl synthetase (AlaRS) which incorporate the L-Ala onto the $tRNA^{Ala}$ and the reaction catalyzed by FemX which transfer the L-Alanyl residue from $tRNA^{Ala}$ to UDP-MurNAc-pentapeptide (UM5K). (**B**) Schematic representation of the hemi-synthesis of L-Ala-$Helix^{Ala}$ used in this study (**C**) Structure of $tRNA^{Ala}$ and the 24- and 8-nt helices that mimic the acceptor arm of $tRNA^{Ala}$. Acceptor arm positions are highlighted in gray.

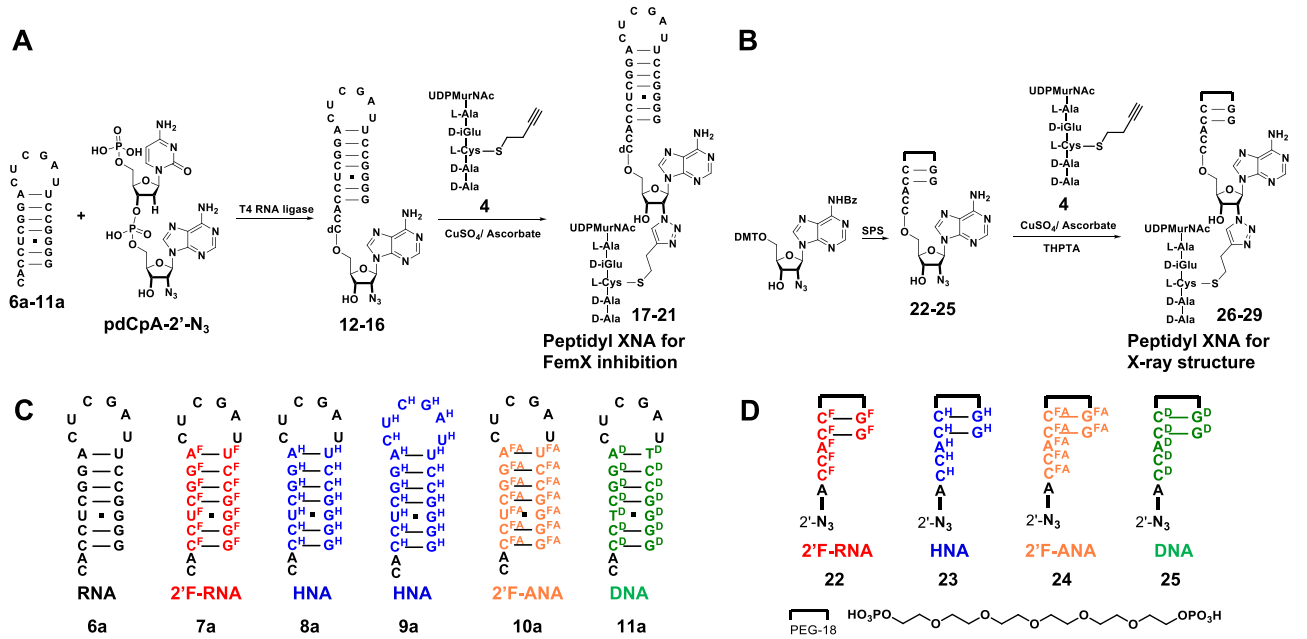

Figure 3. (**A**) Chemical strategy for the synthesis of the 24-nt peptidyl-oligonucleotide bi-substrate analog. (**B**) Chemical strategy for the synthesis of the 8-nt peptidyl-oligonucleotide bi-substrate analogs. (**C**) Helices mimicking the acceptor arm of $tRNA^{Ala}$ used in this study. (**D**) 8-nt helices mimicking the terminal part of the acceptor arm of $tRNA^{Ala}$. A, G, C and U are RNA (black). A^F, G^F, C^F and U^F are 2′F-RNA (red). A^{FA}, G^{FA}, C^{FA} and U^{FA} are 2′F-ANA (orange). A^H, G^H, C^H and U^H are HNA (blue). A^D, G^D, C^D and T^D are DNA (green).

HNA, 2′F-ANA or DNA nucleotides) was determined at 21°C in 20 μl of 50 mM ammonium acetate (pH 7.2). After 0, 15, 30, 60, 120, 300 and 1100 min, an aliquot of each reaction mixture was quenched by the addition of an acetic acid solution (0.1%) containing an internal standard of the reaction product, [^{13}C-^{15}N]-L-Ala-UDP-MurNAc-pentapeptide for quantification of the transfer. The velocity of the transfer of the L-alanyl residue from **6b**, **7b**, **8b**, **9b**, **10b** and **11b** to UDP-MurNAc-pentapeptide was calculated using the linear portion of the curves between 0 and 30 min (Insets in Figure 4). Transfer efficiencies (TE) are expressed in min^{-1} and were calculated by dividing the velocity of each reaction by the final product concentration determined at 1100 min (Supplementary information section 8) to avoid bias arising from differences in substrate concentrations from the steps of liga-

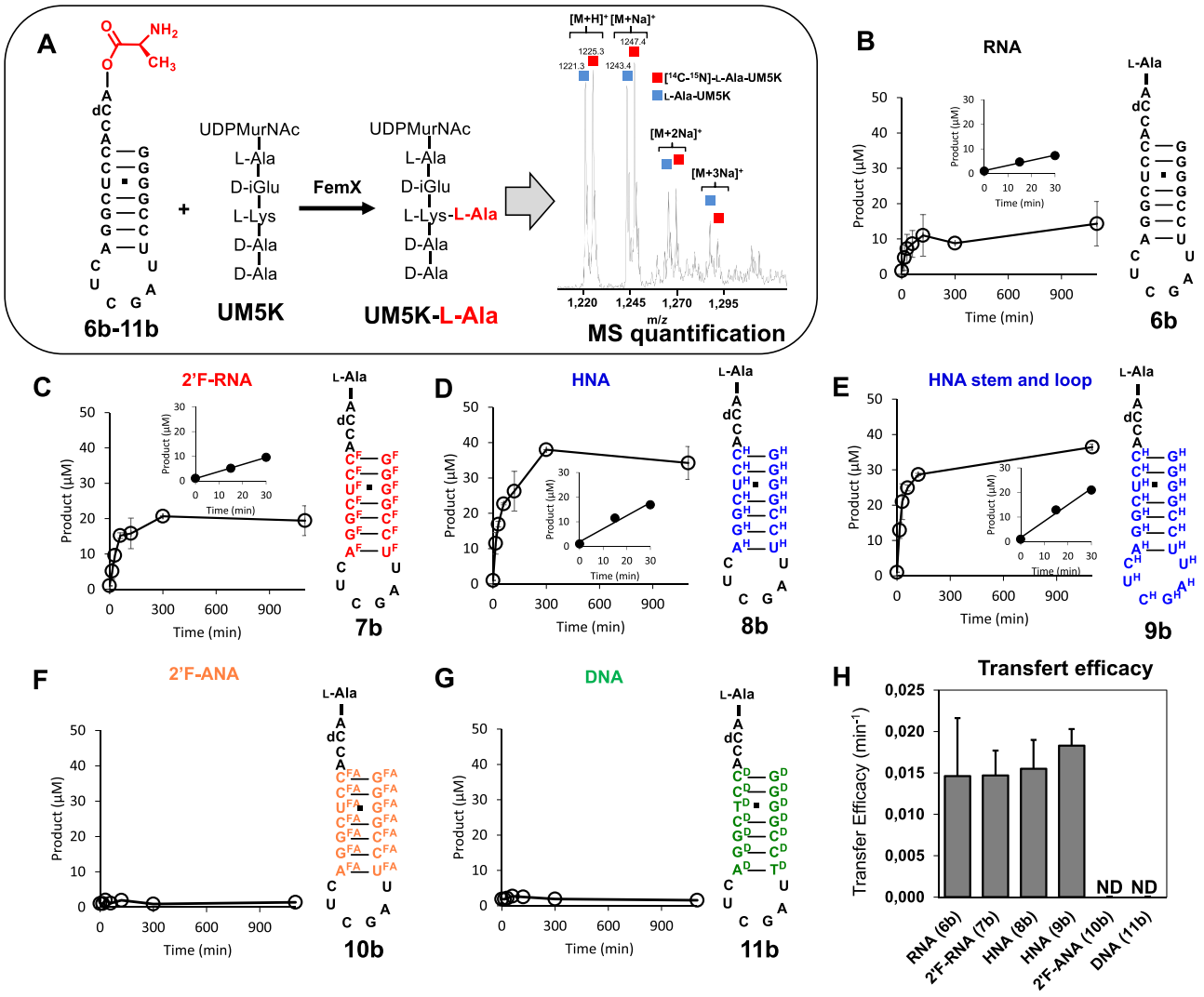

Figure 4. (**A**) Semi-synthesis of L-Ala-tRNA^{Ala} analogs. Kinetics of the transfer of L-Ala from L-Ala-helices and quantification by mass spectroscopy (Supplementary information). Transfer from RNA (**B**) 2′F-RNA (**C**), HNA (**D** and **E**), 2′F-ANA (**F**), or DNA (**G**). (**H**) Transfer efficacy of L-Ala from helices **6b**-**11b** to UM5K by FemX. ND: not detected.

tion, deprotection, and precipitation of the amino-acylated helices.

Synthesis of the alkyne-containing UDP-MurNAc-peptide analogue

Semi-synthesis of the UDP-MurNAc-peptide analogue **4** was performed as previously described (30) (See Supplementary information section 7 and scheme S2 for details).

Synthesis of 24-nt tXNA bi-substrate inhibitors

The convergent synthesis of XNA-containing bi-substrates **17**, **18**, **19**, **20** and **21** (Figure 3A) was based on a CuAAC reaction between alkyne UDP-MurNAc-pentapeptide **4** and 2′-azido XNA-containing oligonucleotide helices **12**, **13**, **14**, **15** and **16**. The 2′-Azido-dinucleotide pdCpA-2′-N_3 was synthesized and ligated to helices **7a**, **8a**, **9a**, **10a** and **11a** using purified T4 RNA ligase (30), with minor modifications (Supplementary information). The resulting 2′-azido helices **12**, **13**, **14**, **15** and **16** were purified by anionic-HPLC and analyzed by HPLC, mass spectrometry (Supplementary information), and denaturing polyacrylamide gel electrophoresis (Supplementary Figure S1 in Supplementary information). Alkyne-containing UDP-MurNAc-pentapeptide **4** was obtained by semi-synthesis using Mur enzymes from *E. coli* (30). The expected bi-substrates **17**, **18**, **19**, **20** and **21** were purified and analyzed by anionic-HPLC and mass spectrometry (Supplementary information).

Synthesis of 8-nt tXNA bi-substrate inhibitors

The 2′-azido-adenosine (A^{76}) at the 3′-extremity of each 8-nt oligonucleotide was introduced by solid-phase synthesis. The 2′-azido-adenosine moiety was used to react with the alkyne containing UDP-MurNAc-pentapeptide **4**, affording compounds **26** (2′F-RNA), **27** (HNA), **28** (2′F-ANA) and **29** (DNA) (Figure 6A). Production of the resin substituted by the 2′-azido nucleotide, the coupling reac-

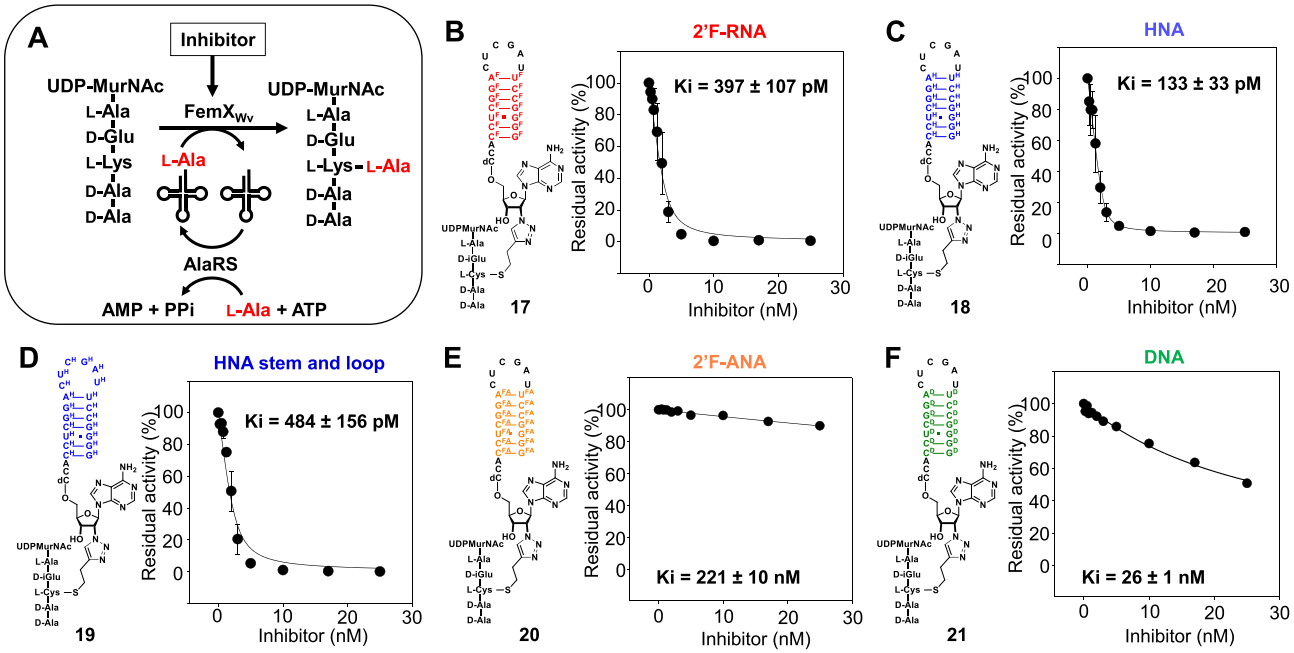

Figure 5. (**A**) Inhibition of FemX by peptidyl-oligonucleotide conjugates containing 2′F-RNA residues in the helix stem (**B**), HNA residues in the helix stem (**C**), HNA residues in the helix stem and loop (**D**), 2′F-ANA residues in the helix stem (**E**) and DNA residues in the helix stem (**F**). K_i values were calculated by fitting the Morrison equation to the data.

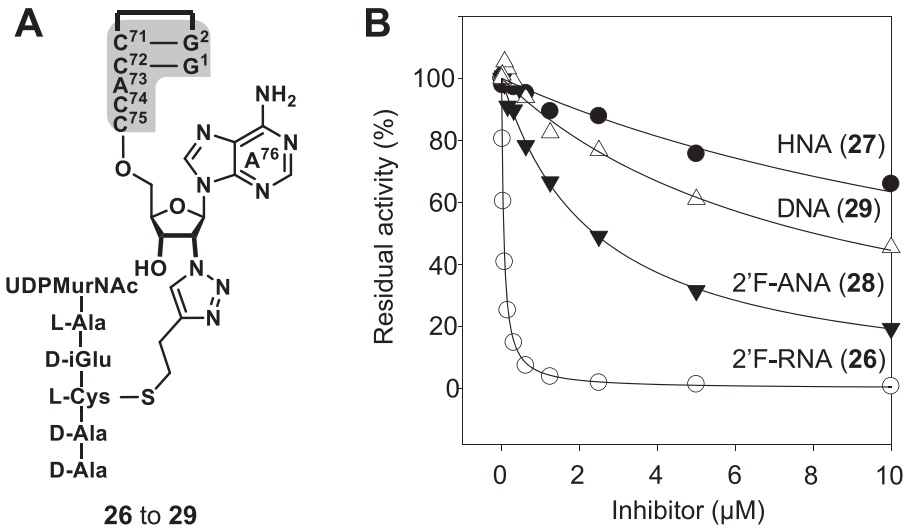

Figure 6. Inhibition of FemX by 8-nt peptidyl-oligonucleotide conjugates. (**A**) General structure of the 8-nt peptidyl-oligonucleotides (in gray: RNA or XNA). (**B**) Inhibition curves of compounds **26** (2′F-RNA), **27** (HNA), **28** (2′F-ANA) and **29** (DNA).

tions, and the final deprotection step were performed as previously described (31). Compounds **26**, **27**, **28** and **29** were purified and analyzed by mass spectrometry (Supplementary information section 11) and anionic-HPLC (Supplementary information section 12).

Ki determination

Inhibition of FemX was tested in a radioactive coupled assay involving [^{14}C]-L-Ala acylation of tRNA^{Ala} by alanyl tRNA synthetase (AlaRS) and transfer of [^{14}C]-L-Ala from the resulting [^{14}C]-L-Ala-tRNA^{Ala} to UDP-MurNAc-L-Ala-γ-D-Glu-L-Lys-D-Ala-D-Ala (UM5K) to form UDP-MurNAc-L-Ala-γ-D-Glu-L-Lys([^{14}C]-L-Ala)-D-Ala-D-Ala ([^{14}C]-L-Ala-UM5K) (Supplementary information section 8) (32).

FemX crystallization, data collection, structure determination and refinement

FemX (255 μM) in complex with peptidyl-XNA **26** to **29** (306 μM) was co-crystallized by sitting-drop vapor

diffusion (Supplementary information). The structures of the complexes were solved by the molecular replacement method at 1.77 Å (HNA), 1.80 Å (2′F-RNA), 1.34 Å (2′F-ANA) and 1.49 Å (DNA) resolution. All complexes include the 337 residues of the protein (see Supplementary information and Supplementary Table S1 for crystal structure determination, data collection and refinement statistics).

RESULTS AND DISCUSSION

Chemical synthesis of Ala-tXNA^{Ala} as an analog of Ala-tRNA^{Ala}

The study of the impact of XNAs on biological systems has been hampered by the difficulties of their synthesis. Although great progress has been made in recent years to obtain XNA-specific polymerases by directed evolution, the enzymatic synthesis of XNAs in significant quantities is still challenging (33,34). Solid-phase synthesis techniques have improved the synthesis of XNA but do not allow the synthesis of large oligonucleotides. Here, we show that an enzymatic ligation catalyzed by T4 RNA ligase between an L-Ala-acylated dinucleotide and an XNA can be used to obtain tXNA^{Ala} analogs. As FemX interacts mainly with the acceptor arm of tRNA^{Ala}, we restricted the size of our XNA probes to 24-nt aminoacylated helices as mimics of the tRNA^{Ala} (35). For this study, we synthesized six helices of 24-nt mimicking the acceptor arm of tRNA^{Ala} (Figure 3C) containing RNA, 2′F-RNA, HNA, 2′F-ANA or DNA, nucleotides in the double stranded portion of the helices (compounds **6a**, **7a**, **8a**, **10a** and **11a**) or HNA in the full helix (compound **9a**). The RNA and DNA helices (**6a** and **11a**, respectively) were synthesized by the phosphoramidite method and purified by anion-exchange chromatography (DNAPac). The XNA helices containing 2′F-RNA, HNA, and 2′F-ANA nucleotides (**7a**, **8a**, **9a**, **10a**) were obtained by solid phase synthesis on an Expedite® 8909 DNA synthesizer (Supplementary information). The acylated dinucleotide (pdCpA-L-alanyl-pentenoyl, Figure 2B) was synthesized (36) and ligated to helices **6a** to **11a** using purified T4 RNA ligase and precipitated using cold ethanol (37). Iodine-mediated L-alanyl deprotection was performed to obtain substrate analogues **6b** to **11b** (29) (Figure 2B).

Transfer efficiency of the amino-acid from Ala-tXNAs

Compounds **6b** to **11b** were used as substrates in an *in vitro* assay to compare the transfer efficiency (TE) of the alanyl residue catalyzed by the enzyme (Figure 4A). We observed similar alanyl transfer in a time-dependent manner with compound **6b** containing natural RNA residues, compound **7b** (2′F-RNA) and compound **8b** (HNA) (TE = 0.015 ± 0.007, 0.015 ± 0.003 and 0.016 ± 0.003 min^{-1}, respectively, Figure 4B–D). The introduction of HNA nucleotides in both the double strand and loop, compound **9b** (Figure 4E) had also no effect on the efficiency of the alanyl transfer compared to the natural RNA (TE = 0.018 ± 0.002 min^{-1}). On the contrary, alanyl transfer from compounds **10b** (2′F-ANA) and **11b** (DNA) was abolished, as we did not detect any product of the reaction by mass spectrometry, even after 1,100 min (Figure 4F and G). These results (Figure 4H) indicates that helices containing HNA or 2′F-RNA are substrates of FemX and 2′F-ANA or DNA in the double strand are unable to sustain the activity of Fem transferase, even if the single-strand terminal part (ACdCA) of the substrates is unmodified.

Synthesis and biological evaluation of helix-based tXNA bi-substrates

Our next objective was to synthesize peptidyl–XNA conjugates as FemX bi-substrate analogs and measure the impact of XNA incorporation in peptidyl–RNA conjugates on the binding of FemX. The peptidyl-XNAs (**17** to **21**) were synthesized in two steps starting from 2′-azido-2′-deoxy-dinucleotides (pdCpA-N_3) (30). First, the 2′-azido-dinucleotide was ligated to helices **7a** to **11a** to afford azido-tXNA **12** to **16** (Figure 3A). The second step used the CuAAC between the azido-tXNA and the alkyne-UDP-MurNAC (compound **4**) to obtain peptidyl-XNAs **17** to **21** (Figure 3A). We have previously shown that the peptidyl UDP-MurNAc-peptide (UM5K) and the RNA helix mimicking the acceptor arm of the tRNA^{Ala} both contribute to high-affinity binding to FemX (30). Inhibition experiments were performed using a coupled enzymatic assay that relies on the aminoacylation of tRNA^{Ala} by the alanyl-tRNA synthetase (AlaRS) and the transfer of the L-alanyl residue from the resulting Ala-tRNA^{Ala} to UM5K by FemX (Figure 5A) (38,39). Compound **17**, which contains 2′F-RNA nucleotides in the double stranded portion of the helix, inhibited FemX, with a K_i of 397 ± 107 pM (Figure 5B), which is in the same order of magnitude to the Ki observed for the inhibition of FemX by peptidyl-RNA (89 ± 10 pM) (30). The introduction of HNA residues in the double strand (compound **18**, Figure 5C) also resulted in inhibition of the same order of magnitude, with a K_i of 133 ± 33 pM. The addition of HNA residues in the helix loop (compounds **19**, Figure 5D) decreased the inhibition of FemX, with a K_i of 484 ± 156 pM. These results show that the introduction of HNA residues in the double strand of the helix did not impact inhibition but that the introduction of HNA in both the double strand and the loop of the helix slightly decreases the inhibition of FemX. Finally, compounds **20** and **21** (Figure 5E and F), containing 2′F-ANA and DNA nucleotides in the double strand of the helix, showed a 2,500-fold (K_i = 221 ± 10 nM) and 300-fold (K_i = 26 ± 1 nM) reduction of inhibition, respectively. These results unambiguously show that the introduction of 2′F-ANA or DNA nucleotides has a deleterious effect on the formation of a stable complex between FemX and the peptidyl-XNA inhibitors.

Synthesis and biological evaluation of minimal peptidyl-tXNA bi-substrate inhibitors for co-crystallization

To study the impact of XNA in the 3′-terminal ACCA part of tRNA^{Ala} we synthesized minimal bi-substrate analogs fully modified by XNA nucleotides (compounds **26** to **29**, Figure 3B). To mimic the terminal part of the acceptor arm of tRNA^{Ala} we chose 8-nt XNA oligonucleotides (Figure 3D), as similar compounds were successful to obtain the crystallographic structure of Fem transferase enzymes in the presence of peptidyl–RNA (32). The synthe-

Table 1. Calculated K_i values deduced by fitting the Morrison equation to the data. Gibbs free enthalpies ΔG° were calculated using the equation $\Delta G^\circ = -RT\ln(K_i)$, with $\underline{R} = 1.987$ cal mol^{-1} K^{-1} and $T = 303.15$ K

Compound composition	K_i (μM)	ΔG° (kcal mol^{-1})	$\Delta\Delta G^\circ$ (kcal mol^{-1})
RNA[(a)]	0.93 ± 0.07	− 8.37	NA
2′F-RNA (**26**)	0.056 ± 0.002	− 10.05	− 1.68
HNA (**27**)	17 ± 1	− 6.60	+1.77
2′F-ANA (**28**)	2.4 ± 0.1	− 7.80	+0.57
DNA (**29**)	8.0 ± 0.6	− 7.07	+1.30

(a) 8-nt peptidyl-RNA (32).

sis of the 8-nt helices (compounds **22** to **25**) was performed by SPS, starting from the 2′-azido 2′-deoxyadenosine attached to a solid support (Figure 3B). A polyethylene glycol linker was incorporated into each oligonucleotide to stabilize the base pairing necessary to conserve good recognition with the enzyme (32) (Figure 3D). Finally, azido-oligonucleotides **22** to **25** were reacted with alkyne containing UDP-MurNAc-pentapeptide **4** through a CuAAC reaction, affording compounds **26** (2′F-RNA), **27** (HNA), **28** (2′F-ANA) and **29** (DNA) (Figure 6A). These short peptidyl-XNAs were tested as inhibitors of FemX (Figure 6B and Table 1). HNA-based molecule **27** inhibited FemX 19-fold less than the peptidyl-RNA analog (K_i = 17 ± 1 μM and 0.93 ± 0.07 μM, respectively). Compounds **28** (2′F-ANA) and **29** (DNA) inhibited FemX moderately less than the RNA analog: 2.6-fold (K_i = 2.4 ± 0.1 μM) and 8.7-fold (K_i = 8.0 ± 0.6 μM), respectively. Interestingly, 2′F-RNA based molecule **26** is the best inhibitor of FemX ($K_i = 0.057 \pm 0.002$ μM) compared to 0.93 ± 0.07 μM obtained for the peptidyl-RNA. These results show that the XNA residues present in the 3′ terminal single-strand portion of the bi-substrate affect ligand binding in the catalytic site of the enzyme. We thus undertook to co-crystallize the four bi-substrate analogs **26** to **29** with the protein to investigate structural determinants that could explain these inhibition variations.

Structural studies of short peptidyl–tXNA bi-substrates in complex with FemX

We determined the crystal structure of FemX bound to compounds **26**, **27**, **28** and **29** (Figure 7). Complex crystals were grown under conditions similar to those used to obtain the complex with our first 8-nt peptidyl–RNA (PDB: 4II9).

Analysis reveals that in the four complexes, the enzyme structure is almost identical to that in the complex with a peptidyl–RNA. R.M.S.D. values between the RNA-based complex and the complexes with compound **26** (2′F-RNA), **27** (HNA), **28** (2′F-ANA) and **29** (DNA) were 0.204, 0.131, 0.144 and 0.116 Å, respectively (including all residues, Supplementary Figure S2). The only minor conformational change observed consisted of a 1.8 Å shift of the Met^{260}–Thr^{264} loop (Supplementary Figure S2) for the two complexes containing the bi-substrates **28** and **29** containing 2′F-ANA and DNA nucleic acids, respectively. This shift could be explained by the loss of the interaction between this loop and the C^{75} and A^{76} nucleotides, which are not correctly positioned to interact with the protein.

The UDP–MurNAc-pentapeptides and the triazole rings in the four complexes were well defined and positioned as in the peptidyl-RNA complex, except for the peptidyl-2′F-RNA **26**, for which the D-iGlu^2 is repositioned (Supplementary Figure S3).

In all four structures, the N_3 of the triazole ring is in the vicinity of the catalytic residue Lys^{305}, which has been shown to directly participate in the chemical step of the transfer reaction (32).

In the peptidyl–RNA complex, only the electron density of the C^{74}C^{75}A^{76} extremity of the oligonucleotides was well defined (Figure 7A). We were able to observe an additional nucleotide (A^{73}) for the HNA, 2′F-ANA and DNA conjugate complexes (Figure 7B–E). Even more interestingly, for the 2′F-RNA:FemX complex, the electron density was sufficiently well defined for positioning all nucleotides (Figure 7C), making it possible to observe for the first time a full peptidyl-helix in complex with a Fem transferase enzyme.

These four complexes allow us to compare the structural features of the different tXNA analogs in interaction with a protein.

For the peptidyl-2′F–RNA (**26**) and peptidyl-HNA (**27**), the nucleotides show productive π-stacking interactions between both A^{73} and C^{74} bases and between C^{74} and C^{75} bases (Supplementary Figure S4A). For the 2′F–RNA complex, we also observe the Watson–Crick base pairing of G^1–C^{72} as well as G^2–C^{71} (Supplementary Figure S4A). We further observed enzyme residues in the vicinity of the C^{71} and C^{72} bases that we had previously identified as major determinants of FemX specificity towards tRNA^{Ala} (Supplementary Figure S4B) (35). For the peptidyl–DNA (**29**) and peptidyl–2′F–ANA (**28**), C^{75} is not well positioned to be in a π-stacking interaction with C^{74}.

We also noted that the positioning of nucleotide A^{76} is different, depending on whether the bi-substrate is an RNA or DNA analogue (Figure 8). The A^{76} adenine is rotated by 159° with 2′F-ANA (**28**) and DNA (**29**) and thus prevents this base from interacting with Ile^{208} and Leu^{301} (Figure 8C and D), as observed for the RNA (PDB 4II9), 2′F-RNA (**26**), and HNA (**27**) complexes (Figure 8A to B). We previously showed that hydrophobic interactions between the A^{76} terminal adenine and Ile^{208} side chain are needed for efficient activity of the Fem enzyme, as substitution of Ile^{208} by an alanine residue led to a 50-fold decrease in turnover number (32). The mispositioning observed for the A^{76} adenine, which carries the L-alanine in the aminoacyl tRNA^{Ala}, might explain why compounds containing 2′F-ANA (**10b**) and DNA (**11b**) are not substrates of FemX (Figure 4) and why the corresponding compounds **20**, **21**, **28** and **29** are not inhibitors of the enzyme (Figures 5 and 6).

Concerning the 1′,5′-anhydrohexitol moiety in compound **27**, the 1.77 Å resolution of the structure allowed us to define, for the first time, the conformation of the HNA sugar and bases in a catalytic site (Supplementary Figure S5). A single structure of a complex between HNA containing oligonucleotide and an archaeal polymerase enzyme has been described but the conformation of the base and the sugar moieties could not be modeled because of insufficient

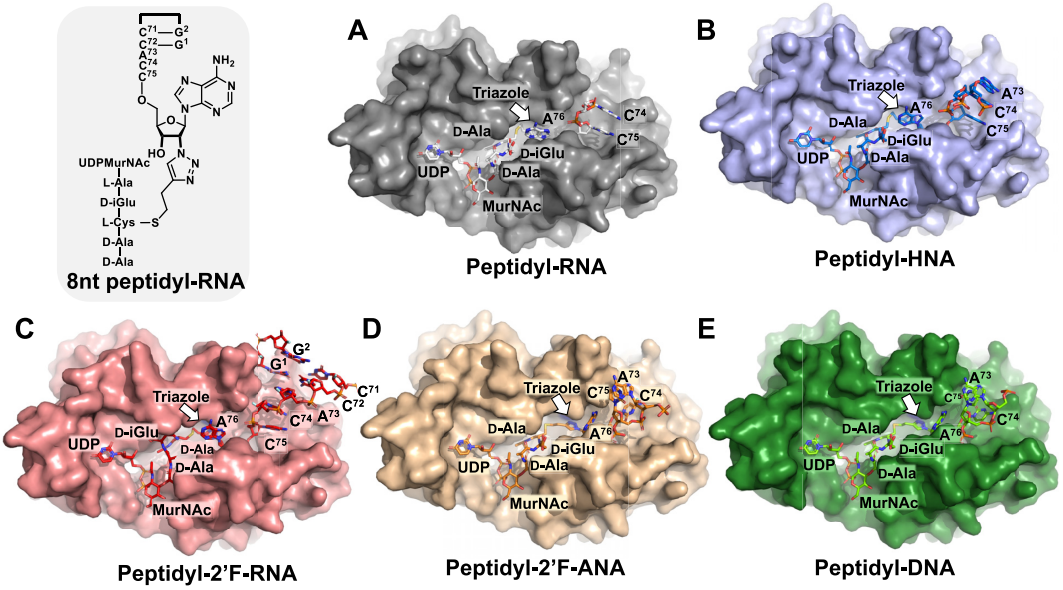

Figure 7. Structures of peptidyl–RNA and peptidyl–XNA bi-substrate analogs in complex with FemX. Protein in complex with bi-substrate containing RNA (**A**), HNA (**B,** compound **27**), 2′F-RNA (**C,** compound **26**), 2′F-ANA (**D,** compound **28**) and DNA (**E,** compound **29**).

resolution (12). In our case, the HNA sugar moiety could be perfectly superposed with the ribose of the RNA, confirming that the 1′,5′-anhydrohexitol of HNA mimics the ribose in its C3′-endo conformation (Figure 8B).

We also explored the interactions of the penultimate C^{75} sugar unit with the Phe^{304} residue conserved in all Fem transferases. This residue was shown to be important for activity, as its substitution by Ala or Leu decreased the FemX turnover number by 16- and 29-fold, respectively (32,39). The distance between 2′F and the phenyl group of Phe^{304} is 3.2 Å in the peptidyl-2′F-RNA compound **26** (Figure 8A), which corresponds to the sum of the Van der Waals radii of the two atoms (3.17Å). The fluorine in compound **26** is at a distance from Phe^{304} that can lead to a lone-pair π stacking interaction (lp–π) (40,41), which was calculated to result in a −1.5 kcal mol^{-1} energy gain (42). This value is compatible with the free energy difference of binding of the RNA and 2′F-RNA compounds, as calculated from their inhibition constants: $K_i^{RNA} = 0.93$ μM ($\Delta G^\circ = -8.37$ kcal mol^{-1}) and $K_i 2'^{F\text{-}RNA} = 0.056$ μM ($\Delta G^\circ = -10.05$ kcal mol^{-1}); $\Delta\Delta G^\circ = -1.68$ kcal mol^{-1}. For the HNA and DNA molecules, the distances between the C2′ position of the C^{75} sugar and the Phe^{304} are 4.7 and 3.6 Å, respectively (Figure 8B and D), and the absence of an electron-rich atom (O or F) on the sugar excludes an lp-π interaction. For compound **28** (2′F-ANA), the distance between the 2′F and Phe^{304} is 4.1 Å (Figure 8C), resulting in a less productive lp–π interaction between the fluorine and phenyl side chain of Phe^{304}. These observations could explain the loss of inhibitory potency of bi-substrates **27**, **28** and **29**, which possess HNA, 2′F-ANA, and DNA at position C^{75} relative to the peptidyl-RNA and the stronger inhibition for compound **26**, which could be due to a stabilizing lp-π interaction between the fluorine pointing towards Phe^{304}.

CONCLUSION

In this study, we designed the first tXNA molecules as substrates or inhibitors of an amino acyl tRNA-dependent enzyme. We show that tXNA can be synthesized using enzymatic ligation with T4 RNA ligase or by solid-phase synthesis. We were able to obtain Ala-$tXNA^{Ala}$ and peptidyl-XNA analogs of different sizes containing XNA in various positions.

We used these tXNA molecules to study the impact of XNA nucleotides on the activity and inhibition of a bacterial Fem transferase enzyme (FemX), as a model of a non-ribosomal peptide synthesis process. We show that the impact of introducing XNA into the tRNA substrate depends on the nature of the XNA, both at the levels of the double-strand and single stranded parts of the $tRNA^{Ala}$. HNA and 2′F-RNA motifs did not significantly modify substrate binding or catalysis, whereas the presence of DNA or 2′F-ANA nucleotides abolished both catalysis and substrate binding.

In terms of modifications in the 3′-ACCA portion of the tRNA, we observed that the 2′F-RNA modification had a more positive impact on recognition by FemX than that with HNA nucleotides. The observed differences rely on the fact that, peptidyl-RNA, -HNA and −2′F-RNA are well positioned in the active site and form more-or-less productive lp-π stacking interactions with the Phe^{304} residue of the protein. The 2′F-ribose of the C^{75} moiety appears to form a very strong interaction with Phe^{304}, resulting in a 16-fold lower inhibition constant than the inhibitor-containing ribonucleotides ($K_i = 0.056$ μM versus 0.93 μM). Our structural data also show for the first time that the geometry of HNA nucleotides is virtually indistinguishable from that of ribonucleotides and that the 1′,5′-anhydrohexitol of HNA can mimic a ribose in its C3′-endo sugar puckering. In contrary, introduction of 2′F-ANA and DNA residues in the

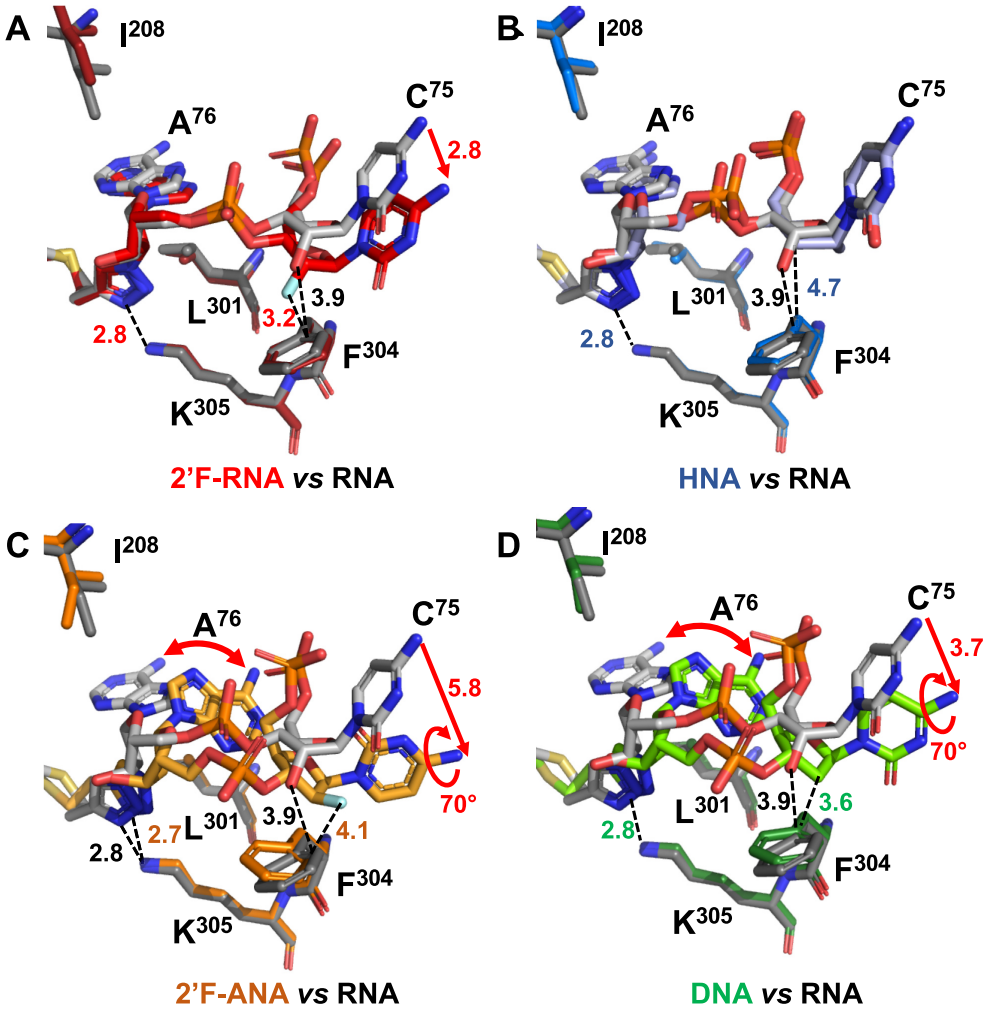

Figure 8. Superposition of the terminal nucleotides C^{75} and A^{76} of the peptidyl-RNA bi–substrate[32] (gray) with the bi-substrates analogues **26** to **29** containing (**A**) 2′F-RNA (red), (**B**) HNA (blue), (**C**) 2′F-ANA (orange) and (**D**) DNA (green), respectively. Red arrows represent rotation or movement of the terminal C^{75} and A^{76} bases.

single strand induced a loss of one π-stacking interaction, leading to poor positioning of the ACCA terminal moiety.

In conclusion, we show here that tXNA molecules can be employed in a non-ribosomal peptidyl enzymatic process and this is the first example of the use of XNA in a functional *in vitro* assay involving protein catalysis. This result paves the way to test tXNA for RNA decoding, which could represent a major step forward in the development of an enzymatically stable translation system. In addition, the observation that tXNA can inhibit enzymes involved in bacterial cell-wall synthesis holds promise for the development of a new class of antibiotics and other tXNAs of therapeutic importance.

DATA AVAILABILITY

The atomic coordinates and structure factors for the reported crystal structures of FemX in complex with compounds **26**, **27**, **28** and **29** and the structural factors reported in this paper have been deposited in the Protein Data Bank, www.pdb.org (accession nos. 7Z6A, 7Z5Y, 7Z6K and 7Z5Z, respectively).

SUPPLEMENTARY DATA

Supplementary Data are available at NAR Online.

ACKNOWLEDGEMENTS

This work was supported by the French Infrastructure for Integrated Structural Biology (FRISBI) ANR-10-INBS-05. Mass spectrometry of unmodified oligonucleotides was made possible by the support of the Hercules Foundation of the Flemish Government (grant 20100225–7). X-ray diffraction data were collected at the SOLEIL Synchrotron (Saint-Aubin, France; PROXIMA-2A and PROXIMA-1 beamlines) and at the ESRF Synchrotron (Grenoble, France; ID23-2 beamline). We thank the beamline staff for their assistance and advice during data collection. This work has benefited from the expertise of the Crystallization Platform of I2BC (Gif-sur-Yvette, France).

FUNDING

French Infrastructure for Integrated Structural Biology (FRISBI) [ANR-10-INBS-05]; Hercules Foundation of the

Flemish Government [20100225-7]. Funding for open access charge: INSERM.
Conflict of interest statement. None declared.

REFERENCES

1. Herdewijn,P. and Marlière,P. (2009) Toward safe genetically modified organisms through the chemical diversification of nucleic acids. *Chem. Biodivers.*, **6**, 791–808.
2. Hendrix,C., Rosemeyer,H., Verheggen,I., Van Aerschot,A., Seela,F. and Herdewijn,P. (1997) 1′, 5′ -Anhydrohexitol oligonucleotides: synthesis, base pairing and recognition by regular oligodeoxyribonucleotides and oligoribonucleotides. *Chem. Eur. J.*, **3**, 110–120.
3. Vandermeeren,M., Préveral,S., Janssens,S., Geysen,J., Saison-Behmoaras,E., Van Aerschot,A. and Herdewijn,P. (2000) Biological activity of hexitol nucleic acids targeted at Ha-ras and intracellular adhesion molecule-1 mRNA. *Biochem. Pharmacol.*, **59**, 655–663.
4. Pezo,V., Liu,W., Abramov,M., Froeyen,M., Herdewijn,P. and Marlière,P. (2013) Binary genetic cassettes for selecting XNA-templated DNA synthesis in vivo. *Angew. Chem. Int. Ed. Eng.*, **125**, 8297–8301.
5. Pinheiro,V.B., Taylor,A.I., Cozens,C., Abramov,M., Renders,M., Zhang,S., Chaput,J.C., Wengel,J., Peak-Chew,S.-Y., McLaughlin,S.H. *et al.* (2012) Synthetic genetic polymers capable of heredity and evolution. *Science*, **336**, 341–344.
6. Eremeeva,E., Fikatas,A., Margamuljana,L., Abramov,M., Schols,D., Groaz,E. and Herdewijn,P. (2019) Highly stable hexitol based XNA aptamers targeting the vascular endothelial growth factor. *Nucleic Acids Res.*, **47**, 4927–4939.
7. Taylor,A.I., Pinheiro,V.B., Smola,M.J., Morgunov,A.S., Peak-Chew,S., Cozens,C., Weeks,K.M., Herdewijn,P. and Holliger,P. (2015) Catalysts from synthetic genetic polymers. *Nature*, **518**, 427–430.
8. Verheggen,I., Van Aerschot,A., Toppet,S., Snoeck,R., Janssen,G., Balzarini,J., De Clercq,E. and Herdewijn,P. (1993) Synthesis and antiherpes virus activity of 1,5-anhydrohexitol nucleosides. *J. Med. Chem.*, **36**, 2033–2040.
9. Lescrinier,E., Esnouf,R., Schraml,J., Busson,R., Heus,H., Hilbers,C. and Herdewijn,P. (2000) Solution structure of a HNA–RNA hybrid. *Chem. Biol.*, **7**, 719–731.
10. Maier,T., Przylas,I., Strater,N., Herdewijn,P. and Saenger,W. (2005) Reinforced HNA backbone hydration in the crystal structure of a decameric HNA/RNA hybrid. *J. Am. Chem. Soc.*, **127**, 2937–2943.
11. Declercq,R., Aerschot,A.V., Read,R.J., Herdewijn,P. and Meervelt,L.V. (2002) Reinforced HNA backbone hydration in the crystal structure of a decameric HNA/RNA hybrid. *J. Am. Chem. Soc.*, **124**, 928–933.
12. Samson,C., Legrand,P., Tekpinar,M., Rozenski,J., Abramov,A., Holliger,P., Pinheiro,V., Herdewijn,P. and Delarue,M. (2020) Structural studies of HNA substrate specificity in mutants of an archaeal DNA polymerase obtained by directed evolution. *Biomolecules*, **10**, 1647.
13. Guo,F., Li,Q. and Zhou,C. (2017) Synthesis and biological applications of fluoro-modified nucleic acids. *Org. Biomol. Chem.*, **15**, 9552–9565.
14. Erande,N., Gunjal,A.D., Fernandes,M. and Kumar,V.A. (2011) Probing the furanose conformation in the 2′–5′strand of isoDNA: RNA duplexes by freezing the nucleoside conformations. *Chem. Commun.*, **47**, 4007.
15. Martínez-Montero,S., Deleavey,G.F., Kulkarni,A., Martín-Pintado,N., Lindovska,P., Thomson,M., González,C., Götte,M. and Damha,M.J. (2014) Rigid 2′,4′-Difluororibonucleosides: synthesis, conformational analysis, and incorporation into nascent RNA by HCV polymerase. *J. Org. Chem.*, **79**, 5627–5635.
16. Damha,M.J., Wilds,C.J., Noronha,A., Brukner,I., Borkow,G., Arion,D. and Parniak,M.A. (1998) Hybrids of RNA and arabinonucleic acids (ANA and 2′F-ANA) are substrates of ribonuclease H. *J. Am. Chem. Soc.*, **120**, 12976–12977.
17. Wilds,C.J. and Damha,M.J. (2000) 2′-Deoxy-2′-fluoro-beta-D-arabinonucleosides and oligonucleotides (2′F-ANA): synthesis and physicochemical studies. *Nucleic Acids Res.*, **28**, 3625–3635.
18. Denisov,A.Y., Noronha,A.M., Wilds,C.J., Trempe,J-F., Pon,R.T., Gehring,K. and Damha,M.J. (2001) Solution structure of an arabinonucleic acid (ANA)/RNA duplex in a chimeric hairpin: comparison with 2′-fluoro-ANA/RNA and DNA/RNA hybrids. *Nucleic Acids Res.*, **29**, 4284–4293.
19. Iannazzo,L., Laisné,G., Fonvielle,M., Braud,E., Herbeuval,J-P., Arthur,M. and Etheve-Quelquejeu,M. (2015) Synthesis of 3′-Fluoro-tRNA analogues for exploring Non-ribosomal peptide synthesis in bacteria. *ChemBioChem*, **16**, 477–486.
20. Patra,A., Paolillo,M., Charisse,K., Manoharan,M., Rozners,E. and Egli,M. (2012) 2′-Fluoro RNA shows increased watson-crick H-bonding strength and stacking relative to RNA: evidence from NMR and thermodynamic data. *Angew. Chem. Int. Ed. Engl.*, **51**, 11863–11866.
21. Pallan,P.S., Greene,E.M., Jicman,P.A., Pandey,R.K., Manoharan,M., Rozners,E. and Egli,M. (2011) Unexpected origins of the enhanced pairing affinity of 2′-fluoro-modified RNA. *Nucleic Acids Res.*, **39**, 3482–3495.
22. Pallan,P.S., Prakash,T.P., De Leon,A.R. and Egli,M. (2016) Limits of RNA 2′-OH mimicry by fluorine: crystal structure of bacillus halodurans RNase h bound to a 2′-FRNA:DNA hybrid. *Biochemistry*, **55**, 5321–5325.
23. Rietmeyer,L., Fix-Boulier,N., Le Fournis,C., Iannazzo,L., Kitoun,C., Patin,D., Mengin-Lecreulx,D., Ethève-Quelquejeu,M., Arthur,M. and Fonvielle,M. (2021) Partition of $tRNA^{Gly}$ isoacceptors between protein and cell-wall peptidoglycan synthesis in *Staphylococcus aureus*. *Nucleic Acids Res.*, **49**, 684–699.
24. Leibowitz,M.J. and Soffer,R.L. (1969) A soluble enzyme from *escherichiacoli* which catalyzes the transfer of leucine and phenylalanine from tRNA to acceptor proteins. *Biochem. Biophys. Res. Commun.*, **36**, 7.
25. Hebecker,S., Krausze,J., Hasenkampf,T., Schneider,J., Groenewold,M., Reichelt,J., Jahn,D., Heinz,D.W. and Moser,J. (2015) Structures of two bacterial resistance factors mediating tRNA-dependent aminoacylation of phosphatidylglycerol with lysine or alanine. *Proc. Natl. Acad. Sci. USA*, **112**, 10691–10696.
26. Gondry,M., Sauguet,L., Belin,P., Thai,R., Amouroux,R., Tellier,C., Tuphile,K., Jacquet,M., Braud,S., Courçon,M. *et al.* (2009) Cyclodipeptide synthases are a family of tRNA-dependent peptide bond-forming enzymes. *Nat. Chem. Biol.*, **5**, 414–420.
27. Garg,R.P., Gonzalez,J.M. and Parry,R.J. (2006) Biochemical characterization of VlmL, a Seryl-tRNA synthetase encoded by the valanimycin biosynthetic gene cluster. *J. Biol. Chem.*, **281**, 26785–26791.
28. Fonvielle,M., Chemama,M., Villet,R., Lecerf,M., Bouhss,A., Valery,J-M., Etheve-Quelquejeu,M. and Arthur,M. (2009) Aminoacyl-tRNA recognition by the $femX_{Wv}$ transferase for bacterial cell wall synthesis. *Nucleic Acids Res.*, **37**, 1589–1601.
29. Lodder,M., Wang,B. and Hecht,S.M. (2005) The N-pentenoyl protecting group for aminoacyl-tRNAs. *Methods*, **36**, 245–251.
30. Fonvielle,M., Mellal,D., Patin,D., Lecerf,M., Blanot,D., Bouhss,A., Santarem,M., Mengin-Lecreulx,D., Sollogoub,M., Arthur,M. *et al.* (2013) Efficient access to Peptidyl-RNA conjugates for picomolar inhibition of non-ribosomal $femX_{Wv}$ aminoacyl transferase. *Chem. Eur. J.*, **19**, 1357–1363.
31. Fonvielle,M., Bouhss,A., Hoareau,C., Patin,D., Mengin-Lecreulx,D., Iannazzo,L., Sakkas,N., El Sagheer,A., Brown,T., Ethève-Quelquejeu,M. *et al.* (2018) Synthesis of lipid-carbohydrate-peptidyl-RNA conjugates to explore the limits imposed by the substrate specificity of cell wall enzymes on the acquisition of drug resistance. *Chem. Eur. J.*, **24**, 14911–14915.
32. Fonvielle,M., Li de La Sierra-Gallay,I., El-Sagheer,A.H., Lecerf,M., Patin,D., Mellal,D., Mayer,C., Blanot,D., Gale,N., Brown,T. *et al.* (2013) The structure of femx(Wv) in complex with a peptidyl-RNA conjugate: mechanism of aminoacyl transfer from Ala-trna(Ala) to peptidoglycan precursors. *Angew. Chem. Int. Ed. Engl.***52**, 7278–7281.
33. Vastmans,K., Pochet,S., Peys,A., Kerremans,L., Van Aerschot,A., Hendrix,C., Marlière,P. and Herdewijn,P. (2000) Enzymatic incorporation in DNA of 1,5-Anhydrohexitol nucleotides. *Biochemistry*, **39**, 12757–12765.

34. Medina,E., Yik,E.J., Herdewijn,P. and Chaput,J.C. (2021) Functional comparison of laboratory-evolved XNA polymerases for synthetic biology. *ACS Synth. Biol.*, **10**, 1429–1437.
35. Villet,R., Fonvielle,M., Busca,P., Chemama,M., Maillard,A.P., Hugonnet,J-E., Dubost,L., Marie,A., Josseaume,N., Mesnage,S. *et al.* (2007) Idiosyncratic features in tRNAs participating in bacterial cell wall synthesis. *Nucleic Acids Res.*, **35**, 6870–6883.
36. Chemama,M., Fonvielle,M., Villet,R., Arthur,M., Valéry,J-M. and Etheve-Quelquejeu,M. (2007) Stable analogues of Aminoacyl-tRNA for inhibition of an essential step of bacterial cell-wall synthesis. *J. Am. Chem. Soc.*, **129**, 12642–12643.
37. Lodder,M., Golovine,S., Laikhter,A.L., Karginov,V.A. and Hecht,S.M. (1998) Misacylated transfer RNAs having a chemically removable protecting group. *J. Org. Chem.*, **63**, 794–803.
38. Maillard,A.P., Biarrotte-Sorin,S., Villet,R., Mesnage,S., Bouhss,A., Sougakoff,W., Mayer,C. and Arthur,M. (2005) Structure-Based site-directed mutagenesis of the UDP-MurNAc-Pentapeptide-Binding cavity of the FemX alanyl transferase from *Weissellavi ridescens*. *J. Bacteriol.*, **187**, 3833–3838.
39. Biarrotte-Sorin,S., Maillard,A.P., Delettré,J., Sougakof,W., Arthur,M. and Mayer,C. (2004) Crystal structures of *weissellaviridescens* FemX and its complex with UDP-MurNAc-Pentapeptide: insights into FemABX family substrates recognition. *Structure*, **12**, 257–267.
40. Auffinger,P., Hays,F.A., Westhof,E. and Ho,P.S. (2004) Halogen bonds in biological molecules. *Proc. Natl. Acad. Sci. U.S.A.*, **101**, 16789–16794.
41. Mooibroek,T.J., Gamez,P. and Reedijk,J. (2008) Lone pair–π interactions: a new supramolecular bond?*Cryst. Eng. Comm.*, **10**, 1501.
42. Chawla,M., Chermak,E., Zhang,Q., Bujnicki,J.M., Oliva,R. and Cavallo,L. (2017) Occurrence and stability of lone pair–π stacking interactions between ribose and nucleobases in functional RNAs. *Nucleic Acids Res.*, **45**, 11019–11032.